

**A measurement of the ratio of inclusive cross sections
 $\sigma(p\bar{p} \rightarrow Z + b\text{jet})/\sigma(p\bar{p} \rightarrow Z + \text{jet})$ at $\sqrt{s} = 1.96$ TeV**

V.M. Abazov,³⁵ B. Abbott,⁷² B.S. Acharya,²⁹ M. Adams,⁴⁸ T. Adams,⁴⁶ G.D. Alexeev,³⁵ G. Alkhalaf,³⁹ A. Alton,^{a,60} G. Alverson,⁵⁹ G.A. Alves,² L.S. Ancu,³⁴ M. Aoki,⁴⁷ Y. Arnaud,¹⁴ M. Arov,⁵⁷ A. Askew,⁴⁶ B. Åsman,⁴⁰ O. Atramentov,⁶⁴ C. Avila,⁸ J. BackusMayer,⁷⁹ F. Badaud,¹³ L. Bagby,⁴⁷ B. Baldin,⁴⁷ D.V. Bandurin,⁴⁶ S. Banerjee,²⁹ E. Barberis,⁵⁹ P. Baringer,⁵⁵ J. Barreto,² J.F. Bartlett,⁴⁷ U. Bassler,¹⁸ V. Bazterra,⁴⁸ S. Beale,⁶ A. Bean,⁵⁵ M. Begalli,³ M. Begel,⁷⁰ C. Belanger-Champagne,⁴⁰ L. Bellantoni,⁴⁷ S.B. Beri,²⁷ G. Bernardi,¹⁷ R. Bernhard,²² I. Bertram,⁴¹ M. Besançon,¹⁸ R. Beuselinck,⁴² V.A. Bezzubov,³⁸ P.C. Bhat,⁴⁷ V. Bhatnagar,²⁷ G. Blazey,⁴⁹ S. Blessing,⁴⁶ K. Bloom,⁶³ A. Boehnlein,⁴⁷ D. Boline,⁶⁹ T.A. Bolton,⁵⁶ E.E. Boos,³⁷ G. Borissov,⁴¹ T. Bose,⁵⁸ A. Brandt,⁷⁵ O. Brandt,²³ R. Brock,⁶¹ G. Brooijmans,⁶⁷ A. Bross,⁴⁷ D. Brown,¹⁷ J. Brown,¹⁷ X.B. Bu,⁴⁷ M. Buehler,⁷⁸ V. Buescher,²⁴ V. Bunichev,³⁷ S. Burdin,^{b,41} T.H. Burnett,⁷⁹ C.P. Buszello,⁴⁰ B. Calpas,¹⁵ E. Camacho-Pérez,³² M.A. Carrasco-Lizarraga,⁵⁵ B.C.K. Casey,⁴⁷ H. Castilla-Valdez,³² S. Chakrabarti,⁶⁹ D. Chakraborty,⁴⁹ K.M. Chan,⁵³ A. Chandra,⁷⁷ G. Chen,⁵⁵ S. Chevalier-Théry,¹⁸ D.K. Cho,⁷⁴ S.W. Cho,³¹ S. Choi,³¹ B. Choudhary,²⁸ T. Christoudias,⁴² S. Cihangir,⁴⁷ D. Claes,⁶³ J. Clutter,⁵⁵ M. Cooke,⁴⁷ W.E. Cooper,⁴⁷ M. Corcoran,⁷⁷ F. Couderc,¹⁸ M.-C. Cousinou,¹⁵ A. Croc,¹⁸ D. Cutts,⁷⁴ M. Cwiok,³⁰ A. Das,⁴⁴ G. Davies,⁴² K. De,⁷⁵ S.J. de Jong,³⁴ E. De La Cruz-Burelo,³² F. Déliot,¹⁸ M. Demarteau,⁴⁷ R. Demina,⁶⁸ D. Denisov,⁴⁷ S.P. Denisov,³⁸ S. Desai,⁴⁷ K. DeVaughan,⁶³ H.T. Diehl,⁴⁷ M. Diesburg,⁴⁷ A. Dominguez,⁶³ T. Dorland,⁷⁹ A. Dubey,²⁸ L.V. Dudko,³⁷ D. Duggan,⁶⁴ A. Duperrin,¹⁵ S. Dutt,²⁷ A. Dyshkant,⁴⁹ M. Eads,⁶³ D. Edmunds,⁶¹ J. Ellison,⁴⁵ V.D. Elvira,⁴⁷ Y. Enari,¹⁷ H. Evans,⁵¹ A. Evdokimov,⁷⁰ V.N. Evdokimov,³⁸ G. Facini,⁵⁹ T. Ferbel,⁶⁸ F. Fiedler,²⁴ F. Filthaut,³⁴ W. Fisher,⁶¹ H.E. Fisk,⁴⁷ M. Fortner,⁴⁹ H. Fox,⁴¹ S. Fuess,⁴⁷ T. Gadfort,⁷⁰ A. Garcia-Bellido,⁶⁸ V. Gavrilov,³⁶ P. Gay,¹³ W. Geist,¹⁹ W. Geng,^{15,61} D. Gerbaudo,⁶⁵ C.E. Gerber,⁴⁸ Y. Gershtein,⁶⁴ G. Ginther,^{47,68} G. Golovanov,³⁵ A. Goussiou,⁷⁹ P.D. Grannis,⁶⁹ S. Greder,¹⁹ H. Greenlee,⁴⁷ Z.D. Greenwood,⁵⁷ E.M. Gregores,⁴ G. Grenier,²⁰ Ph. Gris,¹³ J.-F. Grivaz,¹⁶ A. Grohsjean,¹⁸ S. Grünendahl,⁴⁷ M.W. Grünewald,³⁰ F. Guo,⁶⁹ G. Gutierrez,⁴⁷ P. Gutierrez,⁷² A. Haas,^{c,67} S. Hagopian,⁴⁶ J. Haley,⁵⁹ L. Han,⁷ K. Harder,⁴³ A. Harel,⁶⁸ J.M. Hauptman,⁵⁴ J. Hays,⁴² T. Head,⁴³ T. Hebbeker,²¹ D. Hedin,⁴⁹ H. Hegab,⁷³ A.P. Heinson,⁴⁵ U. Heintz,⁷⁴ C. Hensel,²³ I. Heredia-De La Cruz,³² K. Herner,⁶⁰ G. Hesketh,⁵⁹ M.D. Hildreth,⁵³ R. Hirosky,⁷⁸ T. Hoang,⁴⁶ J.D. Hobbs,⁶⁹ B. Hoeneisen,¹² M. Hohlfeld,²⁴ S. Hossain,⁷² Z. Hubacek,^{10,18} N. Huske,¹⁷ V. Hynek,¹⁰ I. Iashvili,⁶⁶ R. Illingworth,⁴⁷ A.S. Ito,⁴⁷ S. Jabeen,⁷⁴ M. Jaffré,¹⁶ S. Jain,⁶⁶ D. Jamin,¹⁵ R. Jesik,⁴² K. Johns,⁴⁴ M. Johnson,⁴⁷ D. Johnston,⁶³ A. Jonckheere,⁴⁷ P. Jonsson,⁴² J. Joshi,²⁷ A. Juste,^{d,47} K. Kaadze,⁵⁶ E. Kajfasz,¹⁵ D. Karmanov,³⁷ P.A. Kasper,⁴⁷ I. Katsanos,⁶³ R. Kehoe,⁷⁶ S. Kermiche,¹⁵ N. Khalatyan,⁴⁷ A. Khanov,⁷³ A. Kharchilava,⁶⁶ Y.N. Kharzheev,³⁵ D. Khatidze,⁷⁴ M.H. Kirby,⁵⁰ J.M. Kohli,²⁷ A.V. Kozelov,³⁸ J. Kraus,⁶¹ A. Kumar,⁶⁶ A. Kupco,¹¹ T. Kurča,²⁰ V.A. Kuzmin,³⁷ J. Kvita,⁹ S. Lammers,⁵¹ G. Landsberg,⁷⁴ P. Lebrun,²⁰ H.S. Lee,³¹ S.W. Lee,⁵⁴ W.M. Lee,⁴⁷ J. Lellouch,¹⁷ L. Li,⁴⁵ Q.Z. Li,⁴⁷ S.M. Lietti,⁵ J.K. Lim,³¹ D. Lincoln,⁴⁷ J. Linnemann,⁶¹ V.V. Lipaev,³⁸ R. Lipton,⁴⁷ Y. Liu,⁷ Z. Liu,⁶ A. Lobodenko,³⁹ M. Lokajicek,¹¹ P. Love,⁴¹ H.J. Lubatti,⁷⁹ R. Luna-Garcia,^{e,32} A.L. Lyon,⁴⁷ A.K.A. Maciel,² D. Mackin,⁷⁷ R. Madar,¹⁸ R. Magaña-Villalba,³² S. Malik,⁶³ V.L. Malyshev,³⁵ Y. Maravin,⁵⁶ J. Martínez-Ortega,³² R. McCarthy,⁶⁹ C.L. McGivern,⁵⁵ M.M. Meijer,³⁴ A. Melnitchouk,⁶² D. Menezes,⁴⁹ P.G. Mercadante,⁴ M. Merkin,³⁷ A. Meyer,²¹ J. Meyer,²³ N.K. Mondal,²⁹ G.S. Muanza,¹⁵ M. Mulhearn,⁷⁸ E. Nagy,¹⁵ M. Naimuddin,²⁸ M. Narain,⁷⁴ R. Nayyar,²⁸ H.A. Neal,⁶⁰ J.P. Negret,⁸ P. Neustroev,³⁹ S.F. Novaes,⁵ T. Nunnemann,²⁵ G. Obrant,³⁹ J. Orduna,³² N. Osman,⁴² J. Osta,⁵³ G.J. Otero y Garzón,¹ M. Owen,⁴³ M. Padilla,⁴⁵ M. Pangilinan,⁷⁴ N. Parashar,⁵² V. Parihar,⁷⁴ S.K. Park,³¹ J. Parsons,⁶⁷ R. Partridge,^{c,74} N. Parua,⁵¹ A. Patwa,⁷⁰ B. Penning,⁴⁷ M. Perfilov,³⁷ K. Peters,⁴³ Y. Peters,⁴³ G. Petrillo,⁶⁸ P. Pétrouff,¹⁶ R. Piegai,¹ J. Piper,⁶¹ M.-A. Pleier,⁷⁰ P.L.M. Podesta-Lerma,^{f,32} V.M. Podstavkov,⁴⁷ M.-E. Pol,² P. Polozov,³⁶ A.V. Popov,³⁸ M. Prewitt,⁷⁷ D. Price,⁵¹ S. Protopopescu,⁷⁰ J. Qian,⁶⁰ A. Quadt,²³ B. Quinn,⁶² M.S. Rangel,² K. Ranjan,²⁸ P.N. Ratoff,⁴¹ I. Razumov,³⁸ P. Renkel,⁷⁶ P. Rich,⁴³ M. Rijssenbeek,⁶⁹ I. Ripp-Baudot,¹⁹ F. Rizatdinova,⁷³ M. Rominsky,⁴⁷ C. Royon,¹⁸ P. Rubinov,⁴⁷ R. Ruchti,⁵³ G. Safronov,³⁶ G. Sajot,¹⁴ A. Sánchez-Hernández,³² M.P. Sanders,²⁵ B. Sanghi,⁴⁷ A.S. Santos,⁵ G. Savage,⁴⁷ L. Sawyer,⁵⁷ T. Scanlon,⁴² R.D. Schamberger,⁶⁹ Y. Scheglov,³⁹ H. Schellman,⁵⁰ T. Schliephake,²⁶ S. Schlobohm,⁷⁹ C. Schwanenberger,⁴³ R. Schwienhorst,⁶¹ J. Sekaric,⁵⁵ H. Severini,⁷² E. Shabalina,²³ V. Shary,¹⁸ A.A. Shchukin,³⁸ R.K. Shivpuri,²⁸ V. Simak,¹⁰ V. Sirotenko,⁴⁷ P. Skubic,⁷² P. Slattery,⁶⁸ D. Smirnov,⁵³ K.J. Smith,⁶⁶ G.R. Snow,⁶³ J. Snow,⁷¹ S. Snyder,⁷⁰ S. Söldner-Rembold,⁴³ L. Sonnenschein,²¹ A. Sopczak,⁴¹

M. Sosebee,⁷⁵ K. Soustruznik,⁹ B. Spurlock,⁷⁵ J. Stark,¹⁴ V. Stolin,³⁶ D.A. Stoyanova,³⁸ M. Strauss,⁷² D. Strom,⁴⁸ L. Stutte,⁴⁷ L. Suter,⁴³ P. Svoisky,⁷² M. Takahashi,⁴³ A. Tanasijczuk,¹ W. Taylor,⁶ M. Titov,¹⁸ V.V. Tokmenin,³⁵ Y.-T. Tsai,⁶⁸ D. Tsybychev,⁶⁹ B. Tuchming,¹⁸ C. Tully,⁶⁵ P.M. Tuts,⁶⁷ L. Uvarov,³⁹ S. Uvarov,³⁹ S. Uzunyan,⁴⁹ R. Van Kooten,⁵¹ W.M. van Leeuwen,³³ N. Varelas,⁴⁸ E.W. Varnes,⁴⁴ I.A. Vasilyev,³⁸ P. Verdier,²⁰ L.S. Vertogradov,³⁵ M. Verzocchi,⁴⁷ M. Vesterinen,⁴³ D. Vilanova,¹⁸ P. Vint,⁴² P. Vokac,¹⁰ H.D. Wahl,⁴⁶ M.H.L.S. Wang,⁶⁸ J. Warchol,⁵³ G. Watts,⁷⁹ M. Wayne,⁵³ M. Weber,^{9,47} L. Welty-Rieger,⁵⁰ A. White,⁷⁵ D. Wicke,²⁶ M.R.J. Williams,⁴¹ G.W. Wilson,⁵⁵ S.J. Wimpenny,⁴⁵ M. Wobisch,⁵⁷ D.R. Wood,⁵⁹ T.R. Wyatt,⁴³ Y. Xie,⁴⁷ C. Xu,⁶⁰ S. Yacoob,⁵⁰ R. Yamada,⁴⁷ W.-C. Yang,⁴³ T. Yasuda,⁴⁷ Y.A. Yatsunencko,³⁵ Z. Ye,⁴⁷ H. Yin,⁴⁷ K. Yip,⁷⁰ S.W. Youn,⁴⁷ J. Yu,⁷⁵ S. Zelitch,⁷⁸ T. Zhao,⁷⁹ B. Zhou,⁶⁰ J. Zhu,⁶⁰ M. Zielinski,⁶⁸ D. Zieminska,⁵¹ and L. Zivkovic⁶⁷

(The D0 Collaboration*)

¹Universidad de Buenos Aires, Buenos Aires, Argentina

²LAFEX, Centro Brasileiro de Pesquisas Físicas, Rio de Janeiro, Brazil

³Universidade do Estado do Rio de Janeiro, Rio de Janeiro, Brazil

⁴Universidade Federal do ABC, Santo André, Brazil

⁵Instituto de Física Teórica, Universidade Estadual Paulista, São Paulo, Brazil

⁶Simon Fraser University, Vancouver, British Columbia, and York University, Toronto, Ontario, Canada

⁷University of Science and Technology of China, Hefei, People's Republic of China

⁸Universidad de los Andes, Bogotá, Colombia

⁹Charles University, Faculty of Mathematics and Physics,
Center for Particle Physics, Prague, Czech Republic

¹⁰Czech Technical University in Prague, Prague, Czech Republic

¹¹Center for Particle Physics, Institute of Physics,
Academy of Sciences of the Czech Republic, Prague, Czech Republic

¹²Universidad San Francisco de Quito, Quito, Ecuador

¹³LPC, Université Blaise Pascal, CNRS/IN2P3, Clermont, France

¹⁴LPSC, Université Joseph Fourier Grenoble 1, CNRS/IN2P3,
Institut National Polytechnique de Grenoble, Grenoble, France

¹⁵CPPM, Aix-Marseille Université, CNRS/IN2P3, Marseille, France

¹⁶LAL, Université Paris-Sud, CNRS/IN2P3, Orsay, France

¹⁷LPNHE, Universités Paris VI and VII, CNRS/IN2P3, Paris, France

¹⁸CEA, Irfu, SPP, Saclay, France

¹⁹IPHC, Université de Strasbourg, CNRS/IN2P3, Strasbourg, France

²⁰IPNL, Université Lyon 1, CNRS/IN2P3, Villeurbanne, France and Université de Lyon, Lyon, France

²¹III. Physikalisches Institut A, RWTH Aachen University, Aachen, Germany

²²Physikalisches Institut, Universität Freiburg, Freiburg, Germany

²³II. Physikalisches Institut, Georg-August-Universität Göttingen, Göttingen, Germany

²⁴Institut für Physik, Universität Mainz, Mainz, Germany

²⁵Ludwig-Maximilians-Universität München, München, Germany

²⁶Fachbereich Physik, Bergische Universität Wuppertal, Wuppertal, Germany

²⁷Panjab University, Chandigarh, India

²⁸Delhi University, Delhi, India

²⁹Tata Institute of Fundamental Research, Mumbai, India

³⁰University College Dublin, Dublin, Ireland

³¹Korea Detector Laboratory, Korea University, Seoul, Korea

³²CINVESTAV, Mexico City, Mexico

³³FOM-Institute NIKHEF and University of Amsterdam/NIKHEF, Amsterdam, The Netherlands

³⁴Radboud University Nijmegen/NIKHEF, Nijmegen, The Netherlands

³⁵Joint Institute for Nuclear Research, Dubna, Russia

³⁶Institute for Theoretical and Experimental Physics, Moscow, Russia

³⁷Moscow State University, Moscow, Russia

³⁸Institute for High Energy Physics, Protvino, Russia

³⁹Petersburg Nuclear Physics Institute, St. Petersburg, Russia

⁴⁰Stockholm University, Stockholm and Uppsala University, Uppsala, Sweden

⁴¹Lancaster University, Lancaster LA1 4YB, United Kingdom

⁴²Imperial College London, London SW7 2AZ, United Kingdom

⁴³The University of Manchester, Manchester M13 9PL, United Kingdom

⁴⁴University of Arizona, Tucson, Arizona 85721, USA

⁴⁵University of California Riverside, Riverside, California 92521, USA

⁴⁶Florida State University, Tallahassee, Florida 32306, USA

⁴⁷Fermi National Accelerator Laboratory, Batavia, Illinois 60510, USA

⁴⁸University of Illinois at Chicago, Chicago, Illinois 60607, USA

- ⁴⁹Northern Illinois University, DeKalb, Illinois 60115, USA
⁵⁰Northwestern University, Evanston, Illinois 60208, USA
⁵¹Indiana University, Bloomington, Indiana 47405, USA
⁵²Purdue University Calumet, Hammond, Indiana 46323, USA
⁵³University of Notre Dame, Notre Dame, Indiana 46556, USA
⁵⁴Iowa State University, Ames, Iowa 50011, USA
⁵⁵University of Kansas, Lawrence, Kansas 66045, USA
⁵⁶Kansas State University, Manhattan, Kansas 66506, USA
⁵⁷Louisiana Tech University, Ruston, Louisiana 71272, USA
⁵⁸Boston University, Boston, Massachusetts 02215, USA
⁵⁹Northeastern University, Boston, Massachusetts 02115, USA
⁶⁰University of Michigan, Ann Arbor, Michigan 48109, USA
⁶¹Michigan State University, East Lansing, Michigan 48824, USA
⁶²University of Mississippi, University, Mississippi 38677, USA
⁶³University of Nebraska, Lincoln, Nebraska 68588, USA
⁶⁴Rutgers University, Piscataway, New Jersey 08855, USA
⁶⁵Princeton University, Princeton, New Jersey 08544, USA
⁶⁶State University of New York, Buffalo, New York 14260, USA
⁶⁷Columbia University, New York, New York 10027, USA
⁶⁸University of Rochester, Rochester, New York 14627, USA
⁶⁹State University of New York, Stony Brook, New York 11794, USA
⁷⁰Brookhaven National Laboratory, Upton, New York 11973, USA
⁷¹Langston University, Langston, Oklahoma 73050, USA
⁷²University of Oklahoma, Norman, Oklahoma 73019, USA
⁷³Oklahoma State University, Stillwater, Oklahoma 74078, USA
⁷⁴Brown University, Providence, Rhode Island 02912, USA
⁷⁵University of Texas, Arlington, Texas 76019, USA
⁷⁶Southern Methodist University, Dallas, Texas 75275, USA
⁷⁷Rice University, Houston, Texas 77005, USA
⁷⁸University of Virginia, Charlottesville, Virginia 22901, USA
⁷⁹University of Washington, Seattle, Washington 98195, USA
- (Dated: October 29, 2010)

The ratio of the cross section for $p\bar{p}$ interactions producing a Z boson and at least one b quark jet to the inclusive Z + jet cross section is measured using 4.2 fb^{-1} of $p\bar{p}$ collisions collected with the D0 detector at the Fermilab Tevatron collider at $\sqrt{s} = 1.96 \text{ TeV}$. The $Z \rightarrow \ell^+\ell^-$ candidate events with at least one b jet are discriminated from Z + charm and light jet(s) events by a novel technique that exploits the properties of the tracks associated to the jet. The measured ratio is 0.0193 ± 0.0027 for events having a jet with transverse momentum $p_T > 20 \text{ GeV}$ and pseudorapidity $|\eta| \leq 2.5$, which is the most precise to date and is consistent with theoretical predictions.

PACS numbers: 12.38.Qk, 13.85.Qk, 14.65.Fy, 14.70.Hp

The measurement of the production cross section for a Z boson in association with b jets provides an important

test of perturbative quantum chromodynamics (QCD) predictions [1]. A good description of this process by theoretical calculations is essential since it is a major background to searches for the standard model (SM) Higgs boson via $ZH(H \rightarrow b\bar{b})$ associated production [2] and for the supersymmetric partners of b quarks [3]. This process is also sensitive to the b quark density in the proton needed to predict phenomena such as single top quark production [4] and production of non-SM Higgs bosons in association with b quarks [5]. Calculations for the Z boson production in association with b quarks in $p\bar{p}$ colli-

*with visitors from ^aAugustana College, Sioux Falls, SD, USA, ^bThe University of Liverpool, Liverpool, UK, ^cSLAC, Menlo Park, CA, USA, ^dICREA/IFAE, Barcelona, Spain, ^eCentro de Investigacion en Computacion - IPN, Mexico City, Mexico, ^fECFM, Universidad Autonoma de Sinaloa, Culiacán, Mexico, and ^gUniversität Bern, Bern, Switzerland.

sions are available at next-to-leading order (NLO) using two different approaches [1, 6], and they agree within their respective theoretical uncertainties.

In this Letter, we describe a measurement of the ratio of the inclusive cross sections for Z boson production with at least one b quark jet to the $Z + \text{jet(s)}$ production in $p\bar{p}$ interactions, where the Z boson is identified via its $Z \rightarrow ee$ and $Z \rightarrow \mu\mu$ decay modes. The $Z + b$ jet events are separated from Z boson production with light (u , d , or s quarks, or gluons) and charm (c) jet(s) by a discriminant that exploits the properties of the tracks associated to the jet. The measurement of the ratio benefits from cancellations of many systematic uncertainties on the cross sections and therefore allows a more precise comparison with theoretical calculations. Previous measurements by the D0 [7] and CDF [8] collaborations agree with the SM predictions. Here, we present the most precise measurement of the ratio to date. This measurement is a significant improvement over the previous D0 result [7] which utilized 0.18 fb^{-1} of integrated luminosity and assumed the ratio of the $Z + b$ jet cross section to the $Z + c$ jet cross section from NLO calculations. This analysis uses a much larger dataset and a substantially improved method to extract the different jet flavor fractions.

We use data from $p\bar{p}$ collisions at a center-of-mass energy of 1.96 TeV collected by the D0 detector [9] at the Fermilab Tevatron between 2006 and 2009 and corresponding to an integrated luminosity of 4.2 fb^{-1} . The selected events are required to pass at least one of the single electron or single muon triggers. The efficiency of the triggers, as measured from data, is close to 100% (78%) for the $Z \rightarrow ee$ ($Z \rightarrow \mu\mu$) final state.

This analysis relies on all components of the detector: tracking, calorimetry, and muon system and the ability to identify detached vertices. The D0 detector consists of a central tracking system, comprising a silicon microstrip tracker (SMT) and a central fiber tracker, both within a 2 T solenoidal magnet; a liquid-argon and uranium calorimeter, divided into a central calorimeter and two endcap calorimeters; and a muon system, consisting of three layers of tracking detectors and scintillation trigger counters. The SMT allows a precise reconstruction of the $p\bar{p}$ interaction vertex (PV) and of eventual secondary vertices (SV), and an accurate determination of the impact parameter (IP) of a track relative to the PV, which are the key components of the jet lifetime-based b -tagging algorithms.

Offline event selection requires a reconstructed PV that has at least three associated tracks and is located within 60 cm of the center of the detector in the coordinate along the beam direction. The selected events must contain a Z boson candidate with a dilepton invariant mass $70 \text{ GeV} < m_{\ell\ell} < 110 \text{ GeV}$. Throughout this Letter we use Z boson to denote any dilepton event in the above mentioned mass range due to Z or γ^* production.

The dielectron (ee) selection requires at least two electrons of transverse momentum $p_T > 15 \text{ GeV}$ identified by

electromagnetic (EM) showers in the central (with pseudorapidity [10] $|\eta| < 1.1$) or endcap ($1.5 < |\eta| < 2.5$) calorimeter. The showers must have a significant fraction of their energy deposited in the EM calorimeter, be isolated from other energy depositions, and have a shape consistent with that expected for an electron. The central electrons, in addition, must match central tracks or produce electron-like patterns of hits in the tracker.

The dimuon ($\mu\mu$) selection requires at least two muons with segments in the muon spectrometer matched to central tracks with $p_T > 10 \text{ GeV}$ and $|\eta| < 2$. Combined tracking and calorimeter isolation requirements are applied to the muon candidates. Muons from cosmic rays are rejected by applying a timing criterion to the hits in the scintillator layers as well as restricting the position of the muon track with respect to the PV. The two muons must also have opposite electric charges.

A total of 411,064 (224,814) Z boson candidate events are retained in the ee ($\mu\mu$) channel. The $Z + \text{jet}$ sample is then selected by requiring the presence of at least one reconstructed jet with $|\eta| < 2.5$, with the leading jet having $p_T > 20 \text{ GeV}$ and any additional jets having $p_T > 15 \text{ GeV}$. Jets are reconstructed from energy deposits in the calorimeter using the iterative midpoint cone algorithm [11] with a cone of radius 0.5. The energy of jets is corrected for detector response, the presence of noise and multiple $p\bar{p}$ interactions, and the energy deposited outside of the jet cone used for reconstruction. Jets containing b quarks have a different energy response and receive an average additional energy correction of about 6% as determined from simulations. Events with missing transverse energy larger than 60 GeV are rejected to suppress the background from $t\bar{t}$ production. These selection criteria yield a sample of 48,956 (24,450) $Z + \text{jet}$ events in the ee ($\mu\mu$) channel.

Jets considered for b -tagging are subject to a preselection, called taggability, to decouple the intrinsic b jet tagging algorithm performance from other effects. For this purpose, the jet is required to have at least two associated tracks with $p_T > 0.5 \text{ GeV}$, the leading track must have $p_T > 1.0 \text{ GeV}$, and each track must have at least one SMT hit. This requirement has a typical efficiency of 90% per jet. The jet related efficiencies mentioned here and later on are determined from simulations and corrected for the difference observed in data. In order to enrich a sample with heavy-flavor jets, a neural network (NN) based b -tagging algorithm is applied that exploits the longer lifetimes of b -flavored hadrons in comparison to their lighter counterparts [12]. The inputs to the NN combine several characteristic quantities of the jet and associated tracks to provide a continuous output value that tends towards one for b jets and zero for non- b jets. The important input variables are the number of reconstructed SV in the jet, the invariant mass of charged particles associated with the SV (M_{SV}), the number of tracks used to reconstruct the SV, the two-dimensional decay length significance of the SV in the plane transverse to the beam, a weighted combination of the tracks trans-

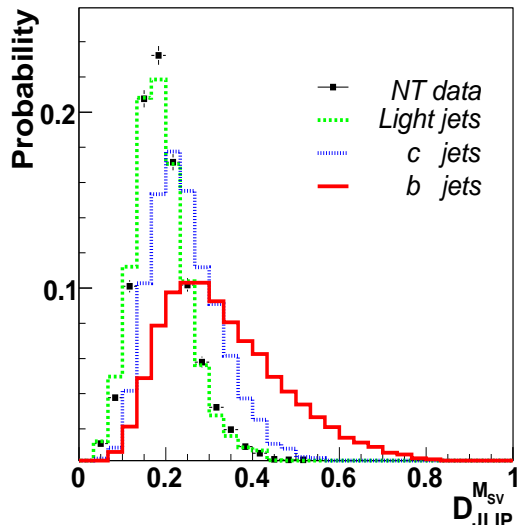


FIG. 1: The probability densities of the $D_{\text{JLIP}}^{M_{\text{SV}}}$ discriminant for b , c and light jets passing the NN b tagging requirement. Also shown is the distribution for the negative tagged (NT) jets in data, described in the text.

verse IP significances, and the probability that the tracks from the jet originate from the PV, which is referred to as the Jet Lifetime Probability (JLIP). We require at least one of the jets in the event to have a NN output greater than 0.5. In the case where the leading jet is not tagged, we apply the NN selection to sub-leading jets. A total of 2,200 (1,015) events with at least one b tagged jet candidate are thus selected in the ee ($\mu\mu$) channel. The tagging efficiency for b jets and the mistagging rate of light jets are parametrized as functions of jet p_T and η , and are about 58% and 2%, respectively, averaged over the kinematics of jets considered in this analysis.

To further separate b jets from c and light jets, we construct a discriminant ($D_{\text{JLIP}}^{M_{\text{SV}}}$) from the combination of M_{SV} and JLIP, $D_{\text{JLIP}}^{M_{\text{SV}}} \equiv (M_{\text{SV}}/10 \text{ GeV} - \ln(\text{JLIP}))/40$. The relative weights of the variables are selected based on studies of simulated data to maximize rejection of c and light quark jets. The mass M_{SV} provides good discrimination between b , c , and light jets due to the different masses of the quarks. Jets from b quarks usually have large values of $-\ln(\text{JLIP})$, while light jets mostly have small values, as their tracks originate from the PV. The average efficiency for the b jets in data to have a well-defined $D_{\text{JLIP}}^{M_{\text{SV}}}$ output is about 68%, which is due to the finite efficiency for a b jet to have a reconstructed SV. Figure 1 shows the normalized distributions of $D_{\text{JLIP}}^{M_{\text{SV}}}$ for jets of different flavors after the NN b tagging requirement. The discriminant $D_{\text{JLIP}}^{M_{\text{SV}}}$ separates well between b , c , and light jets. Figure 1 also shows the $D_{\text{JLIP}}^{M_{\text{SV}}}$ distribution of the tagged jets derived from a light jet enriched data sample, referred to as negatively tagged (NT) data. NT jets have negative values for some of the inputs for the NN algorithm [12] such as decay length significance and IP which are caused by the detector resolution ef-

fects. We estimate the b jet contamination in the NT data using a maximum likelihood fit and subtract its contribution. The template shapes in the corrected NT data and the light jets in Monte Carlo (MC) simulation look similar and the small difference is taken as a systematic uncertainty.

The dominant background to Z + jet production arises from multijet (MJ) events in which jets are misreconstructed as leptons, especially in the ee channel. This instrumental background is estimated from data. We use MJ-enriched data samples that pass all event selection requirements, but fail some of the lepton quality criteria, to determine the kinematic shape of the background distribution. For the ee channel, the MJ sample is obtained by inverting the shower shape requirements and relaxing other identification criteria on the electron candidates. For the $\mu\mu$ channel, the MJ sample consists of events with muon candidates that fail the isolation criteria.

Smaller background contributions arise from top quark pair ($t\bar{t}$) and diboson (WW , WZ , ZZ) production, which contain two leptons in the final state. These backgrounds are estimated using MC simulations with the cross sections rescaled to match theoretical calculations [13, 14]. We simulate inclusive diboson production with PYTHIA [15]. Events from Z +jet and $t\bar{t}$ processes are generated with ALPGEN [16], interfaced with PYTHIA for initial and final state radiation and for hadronization. For these events, a matching procedure is used to avoid double counting of partons produced by ALPGEN and those subsequently added by the showering in PYTHIA. The Z +jets samples consist of Z +light jets and a Z +heavy-flavor component, which includes $Z + b\bar{b}(c\bar{c})$ production. All simulations use the CTEQ6L1 [17] parton distribution functions (PDFs). All samples are processed using a detector simulation based on GEANT3 [18] and the same offline reconstruction algorithms as for data. Events from randomly chosen beam crossings are overlaid on the simulated events to reproduce the effect of multiple $p\bar{p}$ interactions and detector noise. The normalizations of the simulated and the MJ backgrounds are adjusted by scale factors determined from a fit to the $m_{\ell\ell}$ distributions in the inclusive untagged sample. The background fraction in the ee channel is about 18% for both the inclusive untagged and tagged samples, and is dominated by the MJ background. The $\mu\mu$ channel has a higher purity, with a background fraction of only about 0.8% in the untagged and tagged samples.

Corrections are applied to the simulated events to improve the MC modeling. The simulated $Z \rightarrow \mu\mu$ events are weighted with trigger efficiencies measured in data. For the ee channel, no correction is applied as the corresponding trigger is nearly 100% efficient. Lepton identification efficiencies are corrected as a function of η , azimuthal angle ϕ , and the z position of the PV. Jet energies are smeared to reproduce the resolution observed in data, and the efficiency for reconstructing a jet is corrected to match the one in data. The simulated Z boson

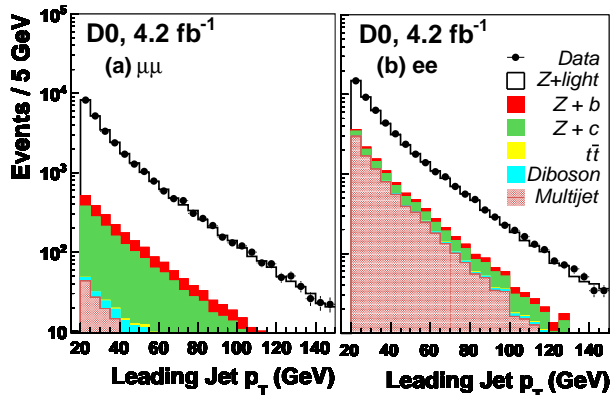


FIG. 2: (color online) The observed p_T distribution of the leading jet in the (a) $\mu\mu$ and (b) ee channel compared with the SM prediction. The uncertainties on the data points are statistical, and the prediction is normalized to the data, as described in the text.

events are reweighted such that the p_T distribution of the Z boson is consistent with the observed distribution. Figures 2(a,b) show the p_T distribution of the leading jet in data compared with the expectation from simulation for Z + jets inclusive events and the associated contributions in each channel. The dominant contribution comes from Z +light jet production.

In order to measure the fraction of events with different jet flavors in the final selected sample, we perform a binned maximum likelihood fit to the $D_{\text{JLIP}}^{M_{\text{SV}}}$ distribution in data using a combination of the light, c , and b flavor jet templates. Before the fit, we subtract the non- $(Z + \text{jet})$ background contributions. A total of 970 (630) events remains in the ee ($\mu\mu$) channel passing all selection requirements and after the background subtraction. The b and c jet $D_{\text{JLIP}}^{M_{\text{SV}}}$ templates are taken from MC simulations with correction factors applied to account for the differences in data and MC efficiencies. The light jet template is obtained from the higher statistics NT data described earlier. The jet flavor fractions obtained in the ee and $\mu\mu$ channels are shown in Table I, where the uncertainties are from the fit due to the data and template statistics. The relative light and c quark fractions are not tightly constrained by the data. The b jet fraction is, however, largely insensitive to variations in the relative amount of light and c jets. Since the individual samples yield consistent results, we combine the ee and $\mu\mu$ samples and remeasure the fractions using an independent fit. The $D_{\text{JLIP}}^{M_{\text{SV}}}$ distributions in the two data samples used for fitting agree after background subtraction. The last column of Table I gives the results of the jet flavor fractions from the combined sample. Figure 3 shows the combined $D_{\text{JLIP}}^{M_{\text{SV}}}$ distribution of b -tagged jets for data along with the fitted contributions from the light (NT data), c and b jets.

The extracted jet flavor fractions are used to determine the ratio $\sigma(Z + b\text{jet})/\sigma(Z + \text{jet})$ as follows:

TABLE I: Jet flavor fractions obtained from template fitting in the dielectron, dimuon and combined channels, along with statistical uncertainties.

Channel	$\mu\mu$	ee	Combined
Events	630	970	1600
$Z + b$	0.248 ± 0.042	0.267 ± 0.036	0.259 ± 0.028
$Z + c$	0.253 ± 0.073	0.364 ± 0.064	0.359 ± 0.049
$Z + \text{light}$	0.499 ± 0.058	0.369 ± 0.049	0.382 ± 0.038

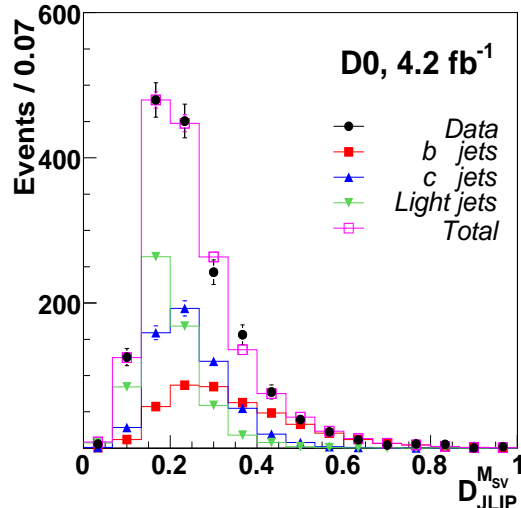


FIG. 3: (color online) The $D_{\text{JLIP}}^{M_{\text{SV}}}$ discriminant distribution of events in the combined sample. The distributions of the b , c , and light jets are weighted by the fractions found from the fit. Uncertainties are statistical only.

$$\frac{\sigma(Z + b\text{jet})}{\sigma(Z + \text{jet})} = \frac{N_b}{N_{\text{incl}} \epsilon_b^{\text{tag}} \epsilon_{b/\text{incl}}^{\text{reco}}}, \quad (1)$$

where N_{incl} is the total number of $Z + \text{jet}$ events before any tagging requirement, N_b is the number of $Z + b\text{jet}$ events obtained from the $D_{\text{JLIP}}^{M_{\text{SV}}}$ fit, ϵ_b^{tag} is the overall $D_{\text{JLIP}}^{M_{\text{SV}}}$ efficiency for b jets, which combines the efficiencies for taggability, NN tagger and $D_{\text{JLIP}}^{M_{\text{SV}}}$ selection, and $\epsilon_{b/\text{incl}}^{\text{reco}}$ accounts for the difference between b and inclusive jet reconstruction efficiencies.

Several experimental uncertainties cancel out in the measurement of $\sigma(Z + b\text{jet})/\sigma(Z + \text{jet})$, including the uncertainties on the luminosity, and trigger, lepton, and some jet identification efficiencies. The two largest remaining sources of systematic uncertainty are uncertainties in the $D_{\text{JLIP}}^{M_{\text{SV}}}$ efficiency and in the shape of the $D_{\text{JLIP}}^{M_{\text{SV}}}$ templates used for the extraction of the b jet fraction. Variation in $D_{\text{JLIP}}^{M_{\text{SV}}}$ efficiency by one standard deviation results in an uncertainty of 3.7% on the final result. The uncertainty due to the shape of the templates (4.2%) is estimated by using an alternate light jet template from

MC, by changing the b quark fragmentation function [15], and by varying the fraction of merged heavy quarks ($b\bar{b}$, $c\bar{c}$) inside the jet. Other important sources of uncertainty are the b tagging efficiency (2.4%), the b jet energy scale (2%), and reconstruction efficiency (3.2%). The total systematic uncertainty on the measurement of the ratio is 7.7%. The final result is

$$\frac{\sigma(Z + b \text{ jet})}{\sigma(Z + \text{ jet})} = 0.0193 \pm 0.0022(\text{stat}) \pm 0.0015(\text{syst}), \quad (2)$$

which is consistent with the ratios obtained separately for the two channels. This measurement is the most precise to date. For the kinematic region considered in the analysis, an NLO MCFM [1] prediction for the ratio yields 0.0192 ± 0.0022 ; this is obtained for the renormalization and factorization scales $Q_R^2 = Q_F^2 = m_Z^2$ (m_Z being the Z boson mass), and with the MSTW2008 PDFs [19]. The prediction decreases by 3.6% when the effects from detector response, resolution as well as hadronization and underlying event are taken into account.

In summary, we have performed the most precise mea-

surement to date of the ratio of the cross section for Z boson production in association with at least one b jet to the inclusive $Z + \text{jet}$ cross section, considering final states with $Z \rightarrow ee$ and $Z \rightarrow \mu\mu$ and jets with $p_T > 20$ GeV and $|\eta| \leq 2.5$. The combined measurement of the ratio yields 0.0193 ± 0.0027 , which is consistent with NLO QCD calculations.

We thank the staffs at Fermilab and collaborating institutions, and acknowledge support from the DOE and NSF (USA); CEA and CNRS/IN2P3 (France); FASI, Rosatom and RFBR (Russia); CNPq, FAPERJ, FAPESP and FUNDUNESP (Brazil); DAE and DST (India); Colciencias (Colombia); CONACyT (Mexico); KRF and KOSEF (Korea); CONICET and UBACyT (Argentina); FOM (The Netherlands); STFC and the Royal Society (United Kingdom); MSMT and GACR (Czech Republic); CRC Program and NSERC (Canada); BMBF and DFG (Germany); SFI (Ireland); The Swedish Research Council (Sweden); and CAS and CNSF (China). We thank the author of MCFM for the help with useful discussion on the theoretical calculations.

-
- [1] J. M. Campbell, R. K. Ellis, F. Maltoni, and S. Willenbrock, *Phys. Rev. D* **69**, 074021 (2004).
- [2] V. M. Abazov *et al.* (D0 Collaboration), *Phys. Rev. Lett.* **104**, 071801 (2010); arXiv:hep-ex/1008.3564; T. Aaltonen *et al.* (CDF Collaboration), *Phys. Rev. D* **80**, 071101 (2009); arXiv:hep-ex/1009.3047.
- [3] V. M. Abazov *et al.* (D0 Collaboration), *Phys. Lett. B* **693**, 95 (2010); T. Aaltonen *et al.* (CDF Collaboration), *Phys. Rev. Lett.* **105**, 081802 (2010).
- [4] V. M. Abazov *et al.* (D0 Collaboration), *Phys. Rev. Lett.* **103**, 092001 (2009); T. Aaltonen *et al.* (CDF Collaboration), *Phys. Rev. Lett.* **103**, 092002 (2009).
- [5] T. Affolder *et al.* (CDF Collaboration), *Phys. Rev. Lett.* **86**, 4472 (2001); V. M. Abazov *et al.* (D0 Collaboration), *Phys. Rev. Lett.* **95**, 151801 (2005); *Phys. Rev. Lett.* **101**, 221802 (2008).
- [6] F. F. Cordero, L. Reina, and D. Wackerroth, *Phys. Rev. D* **78**, 074014 (2008).
- [7] V. M. Abazov *et al.* (D0 Collaboration), *Phys. Rev. Lett.* **94**, 161801 (2005).
- [8] A. Abulencia *et al.* (CDF Collaboration), *Phys. Rev. D* **74**, 032008 (2006); T. Aaltonen *et al.* (CDF Collaboration), *Phys. Rev. D* **79**, 052008 (2009).
- [9] V. M. Abazov *et al.* (D0 Collaboration), *Nucl. Instrum. Methods Phys. Res. Sect. A* **565**, 463 (2006); M. Abolins *et al.*, *Nucl. Instrum. Methods Phys. Res. Sect. A* **584**, 75 (2008); R. Angstadt *et al.*, *Nucl. Instrum. Methods Phys. Res. Sect. A* **622**, 298 (2010).
- [10] Pseudorapidity $\eta = -\ln[\tan(\theta/2)]$ with polar angle θ measured relative to the proton beam direction.
- [11] G. C. Blazey *et al.*, arXiv:hep-ex/0005012.
- [12] V. M. Abazov *et al.* (D0 Collaboration), *Nucl. Instrum. Methods Phys. Res. Sect. A* **620**, 490 (2010).
- [13] N. Kidonakis and R. Vogt, *Phys. Rev. D* **78**, 074005 (2008).
- [14] J. M. Campbell and R. K. Ellis, *Phys. Rev. D* **60**, 113006 (1999).
- [15] T. Sjöstrand, S. Mrenna, and P. Skands, *J. High Energy Phys.* **05**, 026 (2006). Version 6.409 with Tune A is used.
- [16] M. L. Mangano *et al.*, *J. High Energy Phys.* **07**, 001 (2003). Version 2.11 is used.
- [17] J. Pumplin *et al.*, *J. High Energy Phys.* **07**, 012 (2002).
- [18] R. Brun and F. Carminati, CERN Program Library Long Writeup W5013 (1993).
- [19] A. D. Martin, W. J. Stirling, R. S. Thorne, and G. Watt, *Eur. Phys. J. C* **63**, 189 (2009).